Joint Data and Channel Estimation in Radar-enabled Backscatter Communications

Luca Venturino,[†] Emanuele Grossi,[†] Jeremy Johnston,[*] Marco Lops,[§] and Xiaodong Wang[*]
[*]*Department of Electrical Engineering, Columbia University*, New York, NY, USA
[†]*Department of Electrical and Information Engineering, University of Cassino and Southern Lazio*, Cassino, Italy
[§]*Department of Electrical Engineering and Information Technologies, University of Naples "Federico II,"* Naples, Italy
Emails: l.venturino@unicas.it, e.grossi@unicas.it, j.johnston@columbia.edu, lops@unina.it, xw2008@columbia.edu

2023 IEEE International Workshop on Technologies for Defense and Security (TechDefense) | 979-8-3503-1939-2/23/$31.00 ©2023 IEEE | DOI: 10.1109/TechDefense59795.2023.10380821

***Abstract*—In this work, we consider a radar-enabled ambient backscatter communication, where the reverberation generated by a radar system is used as an ambient carrier to deliver information to a destination. Different from a previous study, that focuses on noncoherent encoding/decoding strategies, which require an exhaustive search on a set whose cardinality scales exponentially with the data size, we consider here a pilot-based solution and propose a simplified decoding scheme relying on constrained regularized least squares and search relaxation, whose complexity per iteration scales only linearly with the data size. A numerical example is provided to show merits and drawbacks of the proposed scheme with respect to different benchmarks.**

***Index Terms*—Ambient backscatter, tag, reader, internet of things, radar and communication spectrum sharing, clutter.**

I. Introduction

The exploitation of ambient signals to establish low- or moderate-rate communication links has been fostered by the development of such ideas as Internet-of-Things, smart transportation and automatic driver assistance systems (ADAS) as viable cost-effective solutions, requiring little or no additional physical resources (i.e., bandwidth and power) [2]–[4]. In [1] the idea of exploiting the reverberation generated by a radar system (also known as clutter) has been developed to enable ambient backscatter communications (ABCs). All in all, this study takes advantage of the fact that radar probing signals are inherently periodical, whereby the ambient response, when observed on time intervals in the order of the radar channel coherence time, is itself periodical; this property can be suitably exploited to deliver information from a sender (*tag* in ABC parlance) to a receiver (called *reader*). The study proposes two *Noncoherent* encoding/decoding techniques, therefore not requiring any channel state information (CSI), and demonstrates the feasibility of communication transfer using the radar clutter as carrier signal, thus implementing a simplified and efficient form of radar-communication spectrum sharing at no additional cost.

The work of E. Grossi and L. Venturino was supported by the Italian Ministery of University and Research under the program D.D. n. 104/2022 "Bando PRIN 2022," PE1, project code 202238BJ2R. The work of M. Lops was partially supported by the European Union uner the Italian National Recovery and Resilience Plan (PNRR) of NextGenerationEU, partnership on "Telecommunications of the Future" (PE00000001 – program "RESTART" – E63C22002040007).

The present contribution takes a step forward by considering pilot-assisted radar-enabled communications: pilot symbols are thus inserted in the transmitted frame so as to allow channel estimation and *Coherent* demodulation at the reader. Also, in view of the crucial constraint of cost-effectiveness, a simplified decoding strategy is introduced and assessed, relying on constrained regularized least squares (LS) and search relaxation. Sample plots of the achievable performance, in terms of bit error rate (BER) and root mean square error (RMSE) on the channel estimates are finally offered in order to corroborate the proposed technique.

The paper is organized as follows. In the next section, the system description and the signal model are presented; in Sec. III, the proposed encoding/decoding scheme is illustrated, while a numerical example is provided in Sec. IV to asses the system performance; finally, concluding remarks are given in Sec. V.

Notation: In the following, $\mathbb{C}$ is the set of complex numbers; i is the imaginary unity, while $\Re\{\cdot\}$ denotes real part; $\|\cdot\|$ and $\|\cdot\|_F$ are the Euclidean and the Frobenius norm, respectively; column vectors and matrices are denoted by lowercase and uppercase boldface letters, respectively; $(\cdot)^*$, $(\cdot)^{\mathsf{T}}$, and $(\cdot)^{\mathsf{H}}$ denotes conjugate, transpose, and conjugate-transpose, respectively; $\mathbf{0}_n$ and $\mathbf{1}_n$ are the n-dimensional all-zero and all-one column vector, respectively; $\boldsymbol{I}_n$ is the $n \times n$ identity matrix; $\mathcal{CN}(\mathbf{0}_n, \boldsymbol{C})$ is the complex circularly symmetric Gaussian distribution of an n-dimensional random vector with covariance matrix $\boldsymbol{C}$; $\mathbb{E}[\cdot]$ denotes statistical expectation; $\lceil x \rceil$ the least integer greater than or equal to x; $\Pi(t)$ is a rectangular pulse with unit amplitude and support $[0, 1]$; and $\star$ is the convolution operator.

II. System description

Consider the ambient backscatter communication system in Fig. 1, where a radar monitoring a given region yields a reverberation towards both the tag and the reader, and the tag exploits the incident clutter as an ambient carrier signal to send a message to the reader. The radar emits a periodic passband signal with carrier frequency f_a, bandwidth W_a, and period T_a; for a non-scanning (pulsed or continuous-wave) radar, T_a is the period of the modulating signal or a multiple thereof, while, for a scanning radar, it is the scan-time or a multiple

979-8-3503-1939-2/23/$31.00 ©2023 IEEE

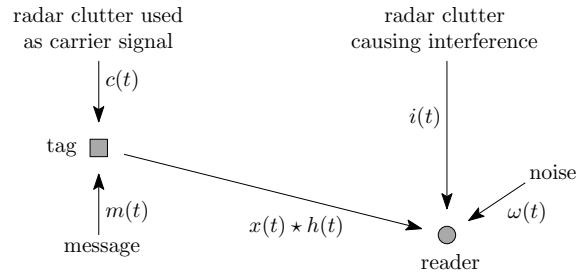

Figure 1. Considered ambient backscatter communication system.

thereof. The tag receives the radar clutter [5], i.e., the unknown echoes produced by the terrain and/or the surrounding objects in response to the signal emitted by the radar, including the possible direct signal from the radar to the tag. Let $c(t)$ and $i(t)$ be the baseband representation of the radar clutter hitting the tag and the reader, respectively, including the possible direct signal.[1] Since the responses of the radar-tag and radar-reader channels are time-invariant over sufficiently short time intervals, upon denoting by L_a the number of radar periods where these channel responses remains stationary, we have that $c(t)$ and $i(t)$ are *locally periodic* signal, meaning that they present L_a approximately-equal cycles within any time segment of length L_aT_a. In the following, we consider the use of $L \leq L_a$ consecutive radar periods, referred to as a frame interval, and we consider the frame interval $[0, LT_a]$ for illustration.

The tag modulates the RF signal $\Re\{c(t)\mathrm{e}^{\mathrm{i}2\pi f_a t}\}$ to send its message $m(t)$ [2]; this is accomplished by switching the antenna load between two or more states, thus altering (in the phase and/or amplitude) the incident waveform every symbol interval $T_s = T_a/N_s$, where N_s is the number of symbols sent over one radar period. We denote by $x_{\ell,n}$ the n-th symbol in the ℓ-th radar period: $x_{\ell,n}$ specifies the complex reflection coefficient of the antenna load employed during the time interval $\big[(\ell N_s + n)T_s, (\ell N_s + n + 1)T_s\big]$ and belongs to the discrete alphabet $\mathcal{X}$. The message over the frame interval can be represented as

$$m(t) = \sum_{\ell=0}^{L-1} \sum_{n=0}^{N_s-1} x_{\ell,n} \Pi\left(\frac{t - (pN_a + n)T_s}{\Delta_s}\right), \quad t \in [0, LT_a], \tag{1}$$

where Δ_s is the symbol duration; we assume that $T_s = \Delta_s + \Delta_g$, where Δ_g is a guard interval between two consecutive transmissions. The baseband representation of the RF signal backscattered by the tag over the frame interval is

$$x(t) = c(t)m(t) = \sum_{\ell=0}^{L} \sum_{n=0}^{N_s-1} x_{\ell,n} c(t) \Pi\left(\frac{t - (\ell N_s + n)T_s)}{\Delta_s}\right) \tag{2}$$

for $t \in [0, LT_a]$; see Fig. 2 for a graphical illustration of $x(t)$.

[1]Even though $c(t)$ and $i(t)$ are produced by the environment in response to the same radar excitation, they are in general different, since tag and reader are in different locations and their antennas have a different orientation and radiation pattern.

The baseband signal received by the reader over the frame interval is

$$z(t) = x(t) \star h(t) + i(t) + \omega(t), \quad t \in [0, LT_a], \tag{3}$$

where $h(t)$ is the baseband impulse response of the channel between the tag and the reader (also accounting for the tag scattering efficiency and any carrier phase offset), which is zero outside $[\tau_h, \tau_h + \Delta_h]$, and $\omega(t)$ is the additive noise. The signal in (3) is passed through a unit-energy low-pass filter $\psi(t)$, with support $[0, \Delta_\psi]$ and bandwidth W_ψ; the corresponding output is, from (2) and (3),

$$\begin{aligned} y(t) = z(t) \star \psi(t) = \sum_{\ell=0}^{L-1} \sum_{n=0}^{N_s-1} x_{\ell,n} \alpha_{\ell,n}(t) + i(t) \star \psi(t) \\ + w(t) \star \psi(t), \quad t \in [0, LT_a], \end{aligned} \tag{4}$$

where $\alpha_{\ell,n}(t) = \big(c(t)\Pi\big((t - (\ell N_s + n)T_s)/\Delta_s\big)\big) \star h(t) \star \psi(t)$ is the unknown received pulse carrying the symbol $x_{\ell,n}$, which is zero outside $[\tau_h + (\ell N_s + n)T_s, \tau_h + (\ell N_s + n)T_s + \Delta_s + \Delta_h + \Delta_\psi]$. To avoid intersymbol interference, the guard interval is chosen to satisfy $\Delta_g \geq \tau_{h,\max} + \Delta_h + \Delta_\psi$, where $\tau_{h,\max}$ is a known upper bound to the delay offsets of the tags. The filtered signal $y(t)$ is sampled at rate K_s/T_s, with $K_s \geq \lceil W_\psi T_s \rceil$, thus obtaining the samples

$$\begin{aligned} y_{\ell,n,k} &= y(t)\big|_{t=\ell T_a + nT_s + kT_s/K_s} \\ &= x_{\ell,n}\alpha_{\ell,n,k} + i_{\ell,n,k} + \omega_{\ell,n,k} \end{aligned} \tag{5}$$

for $\ell = 0, \ldots, L-1$, $n = 0, \ldots, N_s - 1$, and $k = 0, \ldots, K_s - 1$, where $\alpha_{\ell,n,k}$, $i_{\ell,n,k}$, and $\omega_{\ell,n,k}$ are the samples of $\alpha_{\ell,n}(t)$, $i(t) \star \psi(t)$, and $\omega(t) \star \psi(t)$, respectively.

III. Encoding and decoding schemes

Notice that the periodicity of the signals $c(t)$ and $i(t)$ over a frame interval implies that the samples of the pulse carrying the symbols and the corresponding samples $\{i_{\ell,n,1}\}_{\ell=1}^{L-1}$ of the radar interference remain constant, i.e.,

$$\begin{cases} \alpha_{0,n,k} = \cdots = \alpha_{L-1,n,k} = \tilde{\alpha}_{n,k} \\ i_{0,n,k} = \cdots = i_{L-1,n,k} = \tilde{i}_{n,k} \end{cases} \tag{6}$$

for $n = 0, \ldots, N_s - 1$ and $K = 0, \ldots, K_s - 1$, where $\tilde{\alpha}_{n,k}$ and $\tilde{i}_{n,k}$ denote these common values. To take advantage of this signal structure, the samples in (5) are parsed into N_s groups, which define as many time-orthogonal subchannels. Consider now the n-th subchannel, that contains the K observations taken in the n-th symbol interval of each radar period, and organize these samples in the following matrix

$$\begin{aligned} \boldsymbol{Y} &= \begin{bmatrix} y_{0,n,0} & \cdots & y_{0,n,K_s-1} \\ \vdots & & \vdots \\ y_{L-1,n,0} & \cdots & y_{L-1,n,K_s-1} \end{bmatrix} \\ &= \boldsymbol{x}\boldsymbol{\alpha}^{\mathsf{T}} + \mathbf{1}_L \boldsymbol{i}^{\mathsf{T}} + \boldsymbol{\Omega} \in \mathbb{C}^{L \times K_s}, \end{aligned} \tag{7}$$

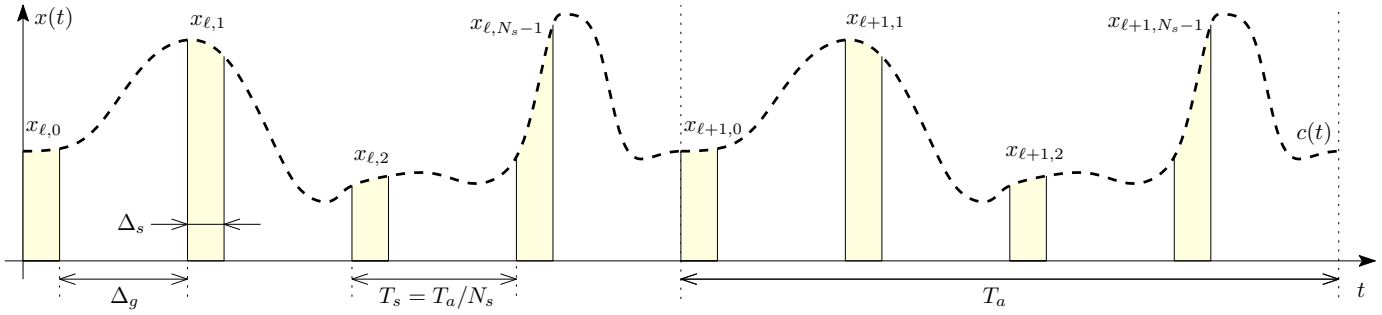

Figure 2. Example of the signal $x(t)$ backscattered by the tag: the symbols $\{x_{\ell,n}\}$ are sent with a linear modulation where the radar clutter $c(t)$ serves as carrier.

where

$$\boldsymbol{x} = \begin{bmatrix} x_{0,n} & \cdots & x_{L-1,n} \end{bmatrix}^{\mathsf{T}} \in \mathcal{X}^L \tag{8a}$$

$$\boldsymbol{\alpha} = \begin{bmatrix} \tilde{\alpha}_{n,0} & \cdots & \tilde{\alpha}_{n,K_s-1} \end{bmatrix}^{\mathsf{T}} \in \mathbb{C}^{K_s} \tag{8b}$$

$$\boldsymbol{i} = \begin{bmatrix} \tilde{i}_{n,0} & \cdots & \tilde{i}_{n,K_s-1} \end{bmatrix}^{\mathsf{T}} \in \mathbb{C}^{K_s} \tag{8c}$$

while $\boldsymbol{\Omega}$ is defined similarly to $\boldsymbol{Y}$. The vector $\boldsymbol{x}$ represents the codeword sent by the tag over L consecutive uses of the n-th subchannel; also, $\boldsymbol{x} = [\boldsymbol{x}_p^{\mathsf{T}} \ \boldsymbol{x}_d^{\mathsf{T}}]^{\mathsf{T}}$, where $\boldsymbol{x}_p$ are P pilot symbols and $\boldsymbol{x}_d$ are D data symbols, with $P + D = L$. Therefore, the transmission rate over this subchannel is

$$R = \frac{D}{L} \log_2 M \tag{9}$$

bits per subchannel-use, where M is the cardinality of $\mathcal{X}$.

The reader must estimate $\boldsymbol{x}_d$ when $\boldsymbol{x}_p$ is known, but $\boldsymbol{\alpha}$ and $\boldsymbol{i}$ are unknown. Assuming that $\boldsymbol{x}_p$ and $\mathbf{1}_P$ are linearly independent, we propose here to jointly estimate $\boldsymbol{x}_d$, $\boldsymbol{\alpha}$, $\boldsymbol{i}$ by solving the following constrained regularized LS problem

$$\min_{\substack{\boldsymbol{x}_d \in \mathcal{X}^D \\ \boldsymbol{\alpha}, \boldsymbol{i} \in \mathbb{C}^{K_s}}} \left\{ \left\| \boldsymbol{Y} - \begin{bmatrix} \boldsymbol{x}_p \boldsymbol{\alpha}^{\mathsf{T}} + \mathbf{1}_P \boldsymbol{i}^{\mathsf{T}} \\ \boldsymbol{x}_d \boldsymbol{\alpha}^{\mathsf{T}} + \mathbf{1}_D \boldsymbol{i}^{\mathsf{T}} \end{bmatrix} \right\|_F^2 + \lambda_x \|\boldsymbol{x}_d\|^2 + \lambda_\alpha \|\boldsymbol{\alpha}\|^2 + \lambda_i \|\boldsymbol{i}\|^2 \right\}, \tag{10}$$

where $\lambda_x, \lambda_\alpha, \lambda_i \geq 0$ are regularization parameters [6].

Problem (10) is quite complex, and we propose here the following suboptimal solution: relax the problem by enlarging the search set over $\boldsymbol{x}_d$ from $\mathcal{X}^D$ to $\mathbb{C}^D$; then, solve the relaxed problem through the block-coordinate descent method (where each *block-variable* is cyclically optimized while leaving the others to their current value); finally, project the relaxed solution onto $\mathcal{X}^D$ to estimate the data (symbol slicing). We consider as block-variables $\boldsymbol{x}_d$ and the pair $[\boldsymbol{\alpha} \ \boldsymbol{i}]$. Then, it can be seen that the minimization over $[\boldsymbol{\alpha} \ \boldsymbol{i}]$ for fixed $\boldsymbol{x}_d$ gives

$$\begin{aligned} \begin{bmatrix} \boldsymbol{\alpha} & \boldsymbol{i} \end{bmatrix} = & \big((\|\boldsymbol{x}_p\|^2 + \|\boldsymbol{x}_d\|^2 + \lambda_\alpha)(L + \lambda_i) \\ & - |\mathbf{1}_P^{\mathsf{T}} \boldsymbol{x}_p + \mathbf{1}_D^{\mathsf{T}} \boldsymbol{x}_d|^2 \big)^{-1} \boldsymbol{Y}^{\mathsf{T}} \begin{bmatrix} \boldsymbol{x}_p^* & \mathbf{1}_P \\ \boldsymbol{x}_d^* & \mathbf{1}_D \end{bmatrix} \\ & \times \begin{bmatrix} L + \lambda_i & -\mathbf{1}_P^{\mathsf{T}} \boldsymbol{x}_p - \mathbf{1}_D^{\mathsf{T}} \boldsymbol{x}_d \\ -\mathbf{1}_P^{\mathsf{T}} \boldsymbol{x}_p^* - \mathbf{1}_D^{\mathsf{T}} \boldsymbol{x}_d^* & \|\boldsymbol{x}_p\|^2 + \|\boldsymbol{x}_d\|^2 + \lambda_\alpha \end{bmatrix} \end{aligned} \tag{11}$$

Algorithm 1 Suboptimal solution to Problem (10)

1: choose $\boldsymbol{x}_d \in \mathbb{C}^D$
2: **repeat**
3: update $\boldsymbol{\alpha}$ and $\boldsymbol{i}$ with (11)
4: update $\boldsymbol{x}_d$ with (12)
5: **until** convergence
6: update $\boldsymbol{x}_d$ by projecting it onto $\mathcal{X}^D$
7: update $\boldsymbol{\alpha}$ and $\boldsymbol{i}$ with (11)
8: **return** $\boldsymbol{x}_d$, $\boldsymbol{\alpha}$, $\boldsymbol{i}$

while the minimization over $\boldsymbol{x}_d$ for fixed $[\boldsymbol{\alpha} \ \boldsymbol{i}]$ gives

$$\boldsymbol{x}_d = \frac{1}{\lambda_x + \|\boldsymbol{\alpha}\|^2} (\boldsymbol{Y}_D - \mathbf{1}_D \boldsymbol{i}^{\mathsf{T}}) \boldsymbol{\alpha}^*, \tag{12}$$

where $\boldsymbol{Y}_D \in \mathbb{C}^{D \times K_s}$ is the matrix obtained by taking the last D rows of $\boldsymbol{Y}$.

The complete routine is reported in Alg. 1. Notice that the computational cost per iteration scales as $\mathcal{O}(LK_s)$; also, since the value of the objective function is not increased at each iteration, the algorithm converges.

IV. Numerical results

Here we evaluate the performance of the proposed pilot-assisted radar-enabled ABC. The tag uses binary symbols, with $\mathcal{X} = \{-1, 1\}$, and the number of samples taken per symbol interval is $K_s = 8$. As a consequence of the linear modulation impressed by the tag (see Fig. 2), only some entries of $\boldsymbol{\alpha}$ are non-zero; here we assume that $\bar{K} = 3$ consecutive samples are non-zero, and we denote by $\bar{\boldsymbol{\alpha}} \in \mathbb{C}^{\bar{K}}$ the sub-vector of $\boldsymbol{\alpha}$ with non-zero entries. The noise received at the reader is modeled as $\boldsymbol{\Omega} \sim \mathcal{CN}(\mathbf{0}_{LK_s}, \sigma_w^2 \boldsymbol{I}_{LK_s})$. The radar-tag-reader and radar-reader channels follows a Rice distribution, which is the typical situation where the clutter is composed of a specular and diffuse component [7]. Specifically, we assume that $\bar{\boldsymbol{\alpha}} = \mu_\alpha \mathrm{e}^{\mathrm{i}\psi_\alpha} \mathbf{1}_{\bar{K}} + \bar{\boldsymbol{\alpha}}_0$ and $\boldsymbol{i} = \mu_i \mathrm{e}^{\mathrm{i}\psi_i} \mathbf{1}_{K_s} + \boldsymbol{i}_0$, where μ_α and μ_i are positive constants, ψ_α, ψ_i are independent random variables uniformly distributed over $[0, 2\pi)$, $\bar{\boldsymbol{\alpha}}_0 \sim \mathcal{CN}(\mathbf{0}_{\bar{K}}, \sigma_\alpha^2 \boldsymbol{I}_{\bar{K}})$ and $\boldsymbol{i}_0 \sim \mathcal{CN}(\mathbf{0}_{K_s}, \sigma_i^2 \boldsymbol{I}_{K_s})$ are independent random vectors, and $\mu_\alpha^2/\sigma_\alpha^2 = \mu_i^2/\sigma_i^2 = 0.1$. The signal-to-noise and signal-to-interference ratios at the reader are $\mathrm{SNR} = (\mu_\alpha^2 + \sigma_\alpha^2)/\sigma_w^2$ and $\mathrm{SIR} = (\mu_\alpha^2 + \sigma_\alpha^2)/(\mu_i^2 + \sigma_i^2)$, respectively.

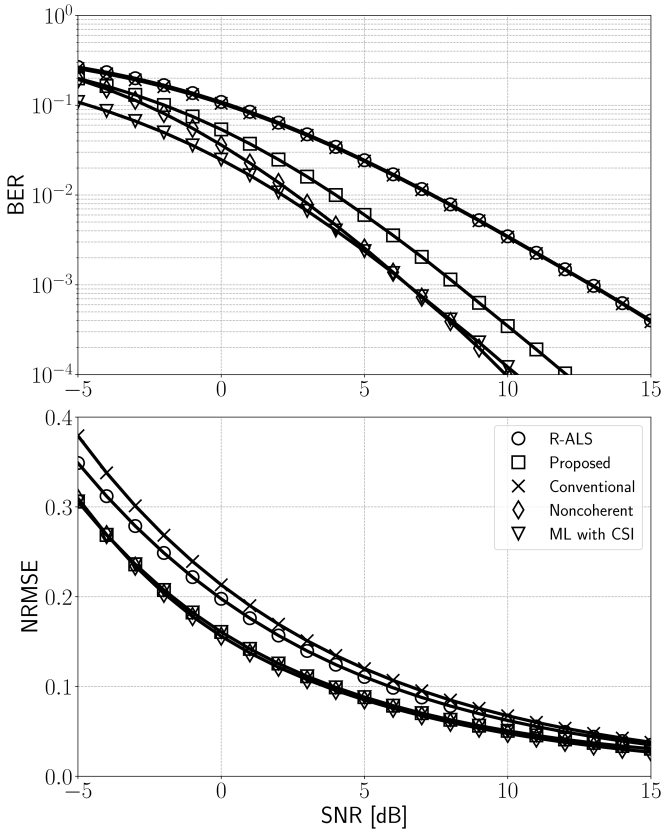

Figure 3. Bit error rate (top) and normalized mean square error (bottom) versus the signal-to-noise ratio when the number of pilots is $P = 4$ and the number of data bits is $D = 4$ (the rate is, therefore, $R = 0.5$ bits/subchannel-use).

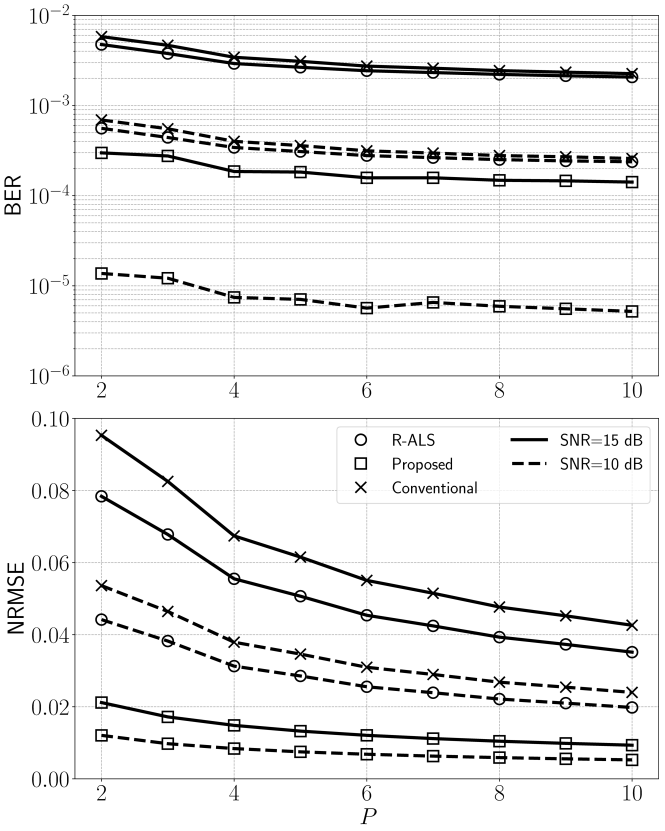

Figure 4. Bit error rate (top) and normalized mean square error (bottom) versus the number of pilots for two signal-to-noise ratios when the number of data bits is 20 times larger than the number of pilots ($D = 20P$; the rate is, therefore, $R = 0.9524$ bits/subchannel-use).

The performance are assessed in terms of BER and normalized RMSE (NRMSE) on the channel estimates, defined as

$$\text{NRMSE} = \sqrt{\frac{\mathbb{E}\left[\|\hat{\boldsymbol{\alpha}} - \boldsymbol{\alpha}\|^2 + \|\hat{\boldsymbol{i}} - \boldsymbol{i}\|^2\right]}{\mathbb{E}\left[\|\boldsymbol{\alpha}\|^2 + \|\boldsymbol{i}\|^2\right]}} \tag{13}$$

where $\mathbb{E}\left[\|\boldsymbol{\alpha}\|^2 + \|\boldsymbol{i}\|^2\right] = \bar{K}(\mu_\alpha^2 + \sigma_\alpha^2) + K_s(\mu_i^2 + \sigma_i^2)$, and $\hat{\boldsymbol{\alpha}}$ and $\hat{\boldsymbol{i}}$ are the estimated channels. For comparison purposes, we consider: the maximum likelihood decoder with perfect channel state information (*ML with CSI*), which represents an upper bound to the performance of any coherent system; the conventional procedure, where the channel is first estimated through the pilots, and then the data is recovered (*Conventional*), which represents the baseline for comparisons; an adapted version of the regularized alternating LS decoding procedure in [8, Alg. 1] (*R-ALS*), that has been used for channel estimation and data detection via a low-rank matrix completion formulation in massive multiple-input multiple-output systems with hybrid analog/digital architectures; and the noncoherent frame-by-frame encoding/decoding rule in [1, Sec. III-A] (*Noncoherent*). The regularization parameters in Problem (10) are set as $\lambda_x = \sigma_w^2$, $\lambda_\alpha = \lambda_i = 0.1$, and all subsequent curves are reported for SIR $= -10\,\text{dB}$.

Fig. 3 shows BER and NRMSE vs SNR when $P = D = 4$, which gives a rate of 0.5 bits/subchannel-use. It can be seen that the proposed scheme largely outperforms the Conventional and the R-ALS, and that it incurs only a small loss (about $2\,\text{dB}$ at BER $= 10^{-4}$) with respect to the Noncoherent scheme and the ML method with perfect CSI. This loss is, however, traded for a gain in terms of computational complexity, which, for fixed rate, scales linearly (with the proposed scheme) rather than exponentially (with the Noncoherent scheme) when the data length D increases: the Noncoherent scheme is, therefore, unfeasible for large values of D, as in the following two figures.

Fig. 4 shows BER and NRMSE vs P for two SNR values when $D = 20P$; the rate is, therefore, 0.9524 bits/subchannel-use. It can be seen that the performance improves with the number of pilots for all the considered schemes, and that the proposed one largely outperforms the Conventional and R-ALS cases. Finally, Fig. 5 shows BER and NRMSE vs D for two SNR values when $P = 3$; when D varies from 1 to 200, the rate increases from 0.25 to 0.9852 bits/subchannel-use. Observe that the performance of the Conventional method is invariant with D; on the contrary, the performance of the other two schemes improves when D increases, since the data symbols are used as *virtual pilots* to improve signal

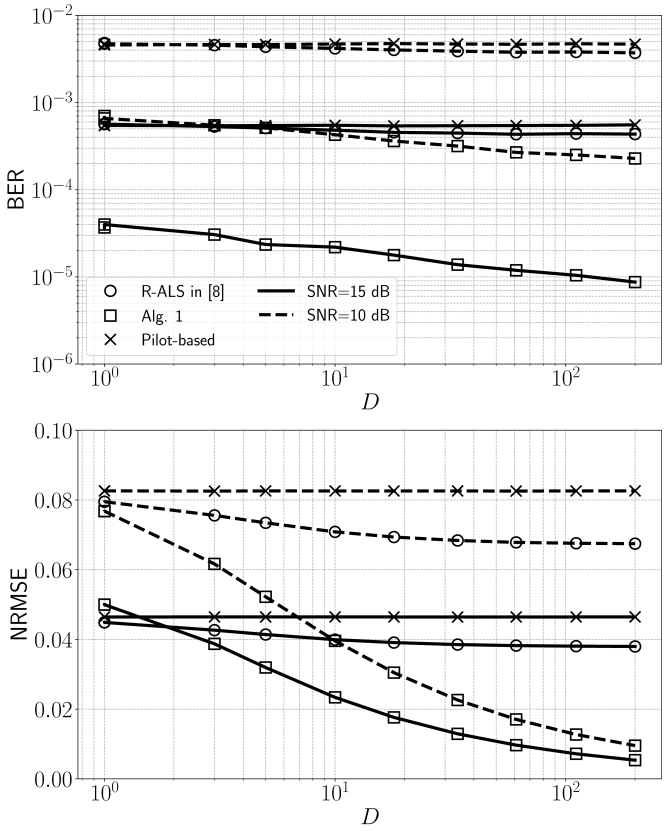

Figure 5. Bit error rate (top) and normalized mean square error (bottom) versus the number of data bits for two signal-to-noise ratios when the number of pilots is $P = 3$ (the rate is, therefore, $R = 0.25, \ldots, 0.9852$ bits/subchannel-use).

recovery. Again, the proposed scheme largely outperforms the Conventional one and the R-ALS method.

V. Conclusion

In this work, we have considered the radar-enabled ABC proposed in [1], where the reverberation generated by a radar system is used as an ambient carrier to deliver information to a destination. Differently from [1], that focuses on noncoherent encoding/decoding strategies requiring exhaustive searches on a set whose cardinality scales exponentially with the data size, we have considered a pilot-based scheme and proposed a simplified decoding scheme relying on constrained regularized LS and search relaxation, whose complexity per iteration scales only linearly with the data size. The considered numerical example has shown that the proposed scheme largely outperforms the Conventional one and the R-ALS, only incurring in a small loss with respect to the Noncoherent system in [1].

References

[1] L. Venturino, E. Grossi, M. Lops, J. Johnston, and X. Wang, "Radar-enabled ambient backscatter communications," *IEEE Transactions on Wireless Communications*, pp. 1–1, 2023.

[2] N. Van Huynh, D. T. Hoang, X. Lu, D. Niyato, P. Wang, and D. I. Kim, "Ambient backscatter communications: A contemporary survey," *IEEE Communications Surveys & Tutorials*, vol. 20, no. 4, pp. 2889–2922, Fourthquarter 2018.

[3] D. C. Nguyen, M. Ding, P. N. Pathirana, A. Seneviratne, J. Li, D. Niyato, O. Dobre, and H. V. Poor, "6G internet of things: A comprehensive survey," *IEEE Internet of Things Journal*, vol. 9, no. 1, pp. 359–383, Jan. 2022.

[4] Z. Feng, Z. Wei, X. Chen, H. Yang, Q. Zhang, and P. Zhang, "Joint communication, sensing, and computation enabled 6G intelligent machine system," *IEEE Network*, vol. 35, no. 6, pp. 34–42, Nov. 2021.

[5] M. I. Skolnik, *Introduction to radar systems*, 3rd ed. New York, NY, USA: McGraw-Hill Higher Education, 2015.

[6] A. Cichocki and R. Zdunek, "Regularized alternating least squares algorithms for non-negative matrix/tensor factorization," in *Advances in Neural Networks – ISNN 2007*, D. Liu, S. Fei, Z. Hou, H. Zhang, and C. Sun, Eds. Berlin, Heidelberg: Springer Berlin Heidelberg, 2007, pp. 793–802.

[7] D. Shnidman, "Generalized radar clutter model," *IEEE Transactions on Aerospace and Electronic Systems*, vol. 35, no. 3, pp. 857–865, Jul. 1999.

[8] S. Liang, X. Wang, and L. Ping, "Semi-blind detection in hybrid massive MIMO systems via low-rank matrix completion," *IEEE Transactions on Wireless Communications*, vol. 18, no. 11, pp. 5242–5254, 2019.